

# Magnetic and Elastic Properties of Ni<sub>49.0</sub>Mn<sub>23.5</sub>Ga<sub>27.5</sub> Premartensite

P. ZHAO, L. DAI, J. CULLEN, and M. WUTTIG

The premartensitic phase transformation in Ni<sub>49.0</sub>Mn<sub>23.5</sub>Ga<sub>27.5</sub> (wt pct) has been established by means of neutron powder diffraction and measurements of elastic constants of  $C_{44}$  and  $C'$ . The commensurate, modulated premartensitic phase has been verified by stiffening of  $C_{44}$  prior to the martensitic phase transformation. The slope change of  $C'$  at the Curie temperature positively confirms that the precursor phenomena in NiMnGa are enhanced by the magnetoelastic coupling. Magnetically, Ni<sub>49.0</sub>Mn<sub>23.5</sub>Ga<sub>27.5</sub> premartensite is characterized by the coexistence of a finite dc magnetic susceptibility and a vanishing magnetocrystalline anisotropy, which distinguishes bcc NiMnGa from the typical magnetic soft materials. This property arises from the competition between the exchange forces of the host lattice and the strong local crystal fields stemming from the tweed.

## I. INTRODUCTION

MATERIALS undergoing a martensitic transformation (MT) exhibit measurable volume and shape changes as the symmetry decreases, *e.g.*, from cubic to tetragonal or orthorhombic. The elastic energy induced by the lattice mismatch between the parent and product phases can be so large that it renders the nucleation of homogeneous martensite energetically unfavorable. It was proposed that the transition is mediated by constrained adaptive phases, which are geometrically close to the martensitic phase and can be treated as a microscopic limit of accommodation of twinning with twin thickness of several atom layers.<sup>[1]</sup> A common feature of bcc solids of MT materials is that the elastic constant  $C'$  is small and keeps softening on approaching the transition. Neutron scattering studies of NiAl display an incipient soft acoustic TA<sub>2</sub> phonon branch above the MT temperature,  $T_M$ , and the corresponding microstructure was identified as tweed using transmission electron diffraction microscopy (TEM).<sup>[2,3]</sup> These observed anomalies prior to MT represent the so-called “precursor phenomena,” which are generally accepted to originate from the electron-phonon coupling and specific nesting features of the Fermi surface.<sup>[4]</sup>

NiMnGa ferromagnetic shape memory alloys (FSMAs) exhibit a large reversible martensitic lattice distortion. Because the alloy is both magnetic and martensitic, it opens the possibility to control the shape memory effect by an external magnetic field, in addition to stress and temperature. Different kinds of modulated structures have been reported<sup>[5]</sup> in the low-temperature martensitic phases upon cooling through  $T_M$ , indicating that the transformation path is composition dependent. It turns out that the electron concentration ( $e/a$ ) controls the stability of the magnetic and crystallographic structures in NiMnGa alloys.<sup>[6,7]</sup> More

intriguingly, it was pointed out that magnetoelastic coupling not only influences MT, but plays a key role in premartensitic transformation as well.<sup>[8,9]</sup> Studies of the lattice dynamics in NiMnGa prior to MT show an incomplete, but more pronounced, softening of phonon frequency of the transverse acoustic phonon branch than that in NiAl, together with a dip at a wave vector  $\xi = 1/3, 1/3, 0$  and narrow [110] ridges of diffuse elastic scattering.<sup>[10,11]</sup> This prominent softening is believed to be enhanced by the coupling between the magnetic and vibrational degrees of freedom in NiMnGa. The incommensurate phase, imaged as short-range strain contrast, the “tweed,” arises from the displacement induced by localized tetragonal perturbations of the cubic lattice. The TEM images indicate that the tweed is comprised of an inhomogeneous assembly of ultrafine locally distorted regions that are randomly distributed in the parent phase.<sup>[10]</sup> For certain compositions, an up-turn of the phonon frequency of the soft mode is observed at a temperature  $T_I$  ( $T_I > T_M$ ), accompanied by an abrupt change of diffuse patterns from diffuse streaking to sharp Bragg-like satellites.<sup>[12]</sup> Both suggest the formation of a modulated premartensitic phase, characterized by a [1/3 1/3 0] modulation along the [110] crystallographic direction of the austenite  $L2_1$  Heusler structure. However, this modulated premartensitic phase can only be observed if the magnetoelastic coupling is strong enough so that the soft phonon is frozen between  $T_I$  and  $T_M$ . The modulation of the premartensitic phase is different from either the five-layer or seven-layer modulation in the low-temperature tetragonal structure.<sup>[13]</sup> This transition is a weakly first-order transformation preceding the formation of martensite, as evidenced by the observation of a small latent heat and magnetic field dependence of the premartensitic transformation temperature  $T_I$ .<sup>[8]</sup> These sequential appearances of austenite, incommensurate phase, commensurate phase, and martensite during cooling have recently been summarized.<sup>[14]</sup>

While there have been extensive theoretical investigations on NiMnGa premartensite, experimental evidence testing those well-established theories<sup>[8,14,15]</sup> is less extensive. This article highlights the elastic and magnetic precursor phenomena in FSMA Ni<sub>49.0</sub>Mn<sub>23.5</sub>Ga<sub>27.5</sub> (wt pct). The results confirm the premartensitic transformation at  $T_I$ , illustrate its magnetoelastic character, and demonstrate

P. ZHAO, Graduate Research Assistant, L. DAI, Research Associate, J. CULLEN, Senior Research Scientist, and M. WUTTIG, Professor, are with the Department of Materials Science and Engineering, University of Maryland, College Park, MD 20742. Contact e-mail: pzhao@wam.umd.edu

This article is based on a presentation made in the symposium entitled “Phase Transformations in Magnetic Materials,” which occurred during the TMS Annual Meeting, March 12–16, 2006, in San Antonio, Texas, under the auspices of the Joint TMS-MPMD and ASMI-MSCTS Phase Transformations Committee.

that the coexistence of a finite magnetic susceptibility and a vanishing magnetic anisotropy in premartensitic state is the signature of the tweed.

## II. EXPERIMENTAL PROCEDURES

$\text{Ni}_{49.0}\text{Mn}_{23.5}\text{Ga}_{27.5}$  (wt pct) single crystals were obtained from AdaptaMat (Helsinki, Finland). The material undergoes a martensitic transformation during cooling at  $T_M = 276$  K and its Curie temperature  $T_C$  is located at 383 K. Powder neutron diffraction data were collected at various temperatures between 227 and 413 K using the high-resolution BT-1 32 detector neutron powder diffractometer at the NIST Center for Neutron Research, Gaithersburg, MD. A Cu(311) monochromator with a 90 deg take-off angle,  $\lambda = 1.5403(2)$  Å, and in-pile collimation of 15' (minutes of arc) was used. A powder sample was sealed in a vanadium container inside a dry He-filled glovebox and a top loading closed cycle refrigerator was used for temperature control. Diffraction data at each temperature were collected over the ranges of 3 to 168 deg  $2\theta$  with a step size of 0.05 deg for approximately 4 hours. The ultrasonic continuous-wave method (UCWM) was used to determine the velocities of  $C_{44}$  elastic waves of a single-crystal specimen vibrating in the hundred kilohertz range. A magnetic field of  $6.4 \times 10^2$  kA/m was applied during the measurement to saturate the specimen. The detailed experimental setup can be found in a previous article.<sup>[16]</sup> The evolution of the internal friction (IF) and elastic constant  $C'$  during heating and cooling was studied by a cantilever oscillation measurement (COM) apparatus. This apparatus has also been previously described.<sup>[17,18]</sup> It should be noted that the relative change of  $C'$  was measured at a frequency of at most kilohertz by COM, much lower than the frequencies used by the UCWM. To perform the magnetic measurements, very thin circular disks with a diameter of 3 mm and a thickness of 0.3 mm were cut with a wire electrical discharge machine at room temperature so that the demagnetization factor is close to 1. The disks were oriented with a (110) normal to contain [001], [110], and [111] directions in the plane and so that the measuring magnetic field could be applied parallel to the circular disk surface and aligned along the desired crystallographic directions. Magnetic measurements were carried out with a superconducting quantum interference device magnetometer. Prior to each measurement, the specimen was heated above its Curie temperature to ensure that each measurement corresponds to the first magnetization process.

## III. RESULTS AND DISCUSSION

Crystal structures at various temperatures as determined by high-resolution neutron powder diffraction are shown in Figure 1. At 413 K,  $\text{Ni}_{49.0}\text{Mn}_{23.5}\text{Ga}_{27.5}$  is in the paramagnetic state. All the Bragg peaks observed could be indexed on a fcc  $L2_1$  Heusler lattice with lattice parameter  $a_c = 5.83$  Å (space group:  $Fm\bar{3}m$ ). On cooling to 313 K, no additional peak appeared. However, pronounced intensity increases were observed at  $2\theta$  positions close to the potential peaks of the low-temperature martensitic phase. The intensity increases indicate the appearance of an intermediate phase, reflecting that the material prepares for the martensitic

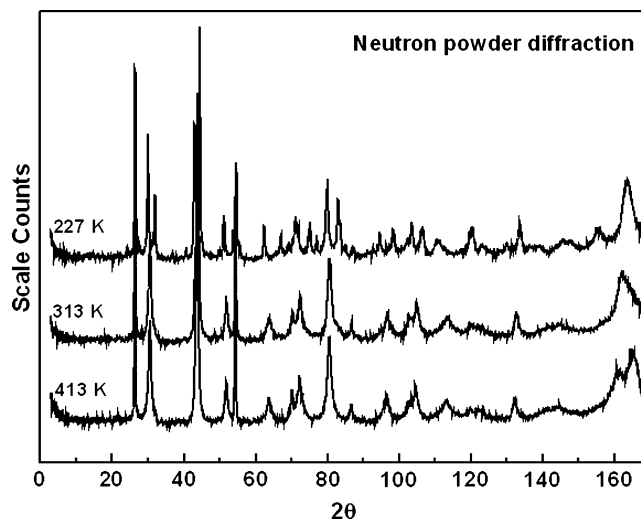
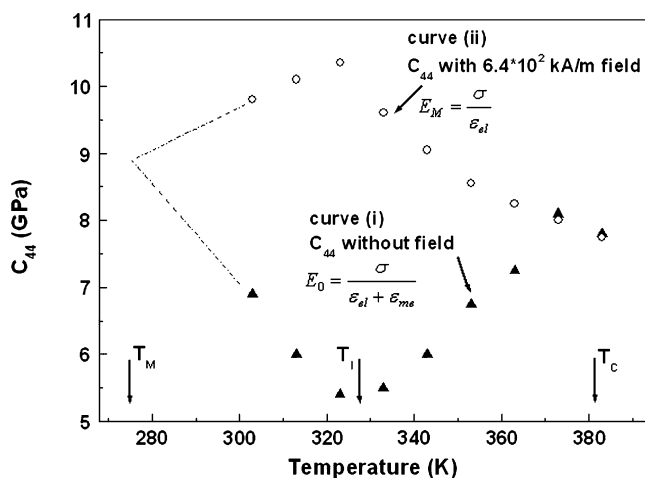


Fig. 1—Neutron powder diffraction patterns of  $\text{Ni}_{49.0}\text{Mn}_{23.5}\text{Ga}_{27.5}$  at 413 K (parent phase), 313 K (premartensitic phase), and 227 K (martensitic phase), respectively.

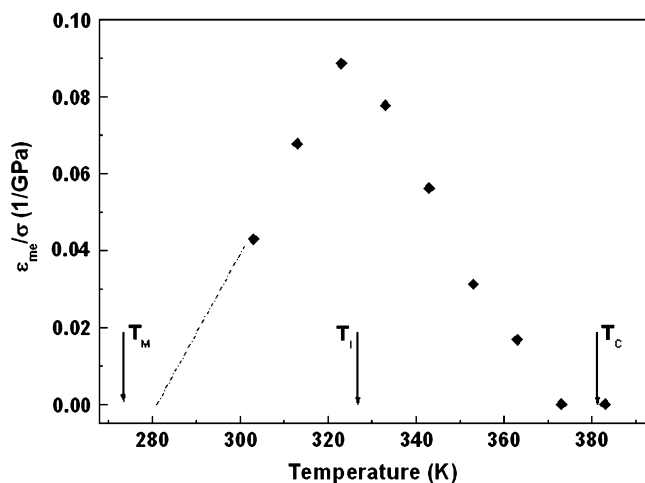
transformation before it actually occurs. Above  $T_M$ , small crystallite size and microstrain contribute to the peak broadening in all the diffraction data measured. The neutron diffraction line-broadening effects were analyzed by means of the Williamson–Hall analysis, which allowed the separation of size and strain parameters. The observed crystallite size varied between 13 and 15 nm, which is close to the coherence length of tweed. The calculated microstrain of the cubic lattice varied from 0.28 to 0.49 pct. Upon cooling the specimen to 227 K, some of the original fcc diffraction peaks split, demonstrating that the material has transformed into a martensitic tetragonal structure (space group:  $I4/mmm$ ). The refined lattice parameters of the tetragonal unit cell are  $a_t = 4.205$  Å,  $c_t = 5.585$  Å ( $c_t/a_t = 1.33$ ). In order to compare them with the parent phase, the tetragonal structures are referenced to the  $L2_1$  cubic coordinates in which case the new lattice parameters are  $a_t = 5.947$  Å and  $c_t = 5.585$  Å ( $c_t/a_t = 0.94$ ). Hence, the lattice distortion due to MT is about 6.1 pct. This tetragonal structure corresponds to the five-layer modulated martensitic structure reported previously.<sup>[19]</sup>

Considering the internal strain that develops on cooling in NiMnGa, it is important to understand the elastic behavior in the vicinity of the phase transformations, because it provides insight into the nature of the transition. The high-frequency elastic constant  $C_{44}$  measured by UCWM clearly demonstrates the presence of a commensurate, modulated phase on cooling between  $T_I$  and  $T_M$ , as illustrated in Figure 2(a). Without applying an external magnetic field, the high frequency  $C_{44}$  exhibits a linear softening between  $T_C$  and  $T_I$  (around 333 K). With further cooling below  $T_I$ ,  $C_{44}$  stiffens as seen in curve (i). The upturn at  $T_I$  reflects that, close to the  $T_M$ , the commensurate phase is more stable than the parent phase. For other compositions of NiMnGa, a similar tendency of the phonon frequency as a function of temperature was reported.<sup>[12]</sup> The unique feature of the softening and subsequent hardening of both the relevant elastic constants and phonon frequency must be attributed to the combination of their magnetic and martensitic nature. Curve (ii)

was measured in the same way except that a  $6.4 \times 10^2$  kA/m magnetic field was applied to the sample. Below  $T_C$ , the temperature dependence of the high-frequency  $C_{44}$  of the magnetically saturated specimen varies completely opposite to the anomalies of the specimen in its nonmagnetized state.  $C_{44}$  keeps increasing between  $T_C$  and  $T_I$ , leading to the classical  $\Delta E$  effect. Specifically, once the spin system in the specimen is aligned by the external field, no magnetoelastic strain but only pure elastic strain can be detected with changing temperature. The magnetoelastic strain  $\varepsilon_{me}$  (actually the ratio  $\varepsilon_{me}/\sigma$  at constant measuring stress  $\sigma$ ) can be numerically calculated from the difference of  $C_{44}$  measured with and without magnetic field, curves (i) and (ii), and plotted in Figure 2(b). It is not surprising to see that  $\varepsilon_{me}$  equals zero above  $T_C$ , because the material is then in its paramagnetic state. However, from the linear extension of the data in Figure 2(b), it seems that  $\varepsilon_{me}$  approaches zero upon cooling the material to  $T_M$  as well. The magnetoelastic strain exhibits a maximum at  $T_I$ , providing clear evidence of magnetoelastic condensation at the incommensurate/commensurate phase



(a)



(b)

Fig. 2—(a) Temperature dependence of the elastic constant  $C_{44}$ : (i) high-frequency  $C_{44}$  measured without applying external magnetic field; and (ii) high-frequency  $C_{44}$  with  $6.4 \times 10^2$  kA/m magnetic field applied. (b) Calculated  $\varepsilon_{me}/\sigma$  as a function of temperature.

transition in agreement with the phonon condensation previously observed by neutron diffraction.<sup>[12]</sup> After the formation of the commensurate phase in the magnetically saturated specimen,  $C_{44}$  decreases with further cooling below  $T_I$ . This softening behavior is not yet fully understood.

The elastic constant  $C'$  is another important parameter to monitor the precursor phenomena in NiMnGa because it is associated with a weak restoring shear of the  $\{110\}$  planes in the  $\langle 1\bar{1}0 \rangle$  directions in the cubic lattice. Figure 3 displays the evolution of the low-frequency  $C'$  and internal friction with cooling and heating above  $T_M$  measured by COM. The relative change of this low-frequency  $C'$  decreases in several linear regimes starting in the high-temperature phases, reflecting the increase of the lattice softening. Within the measuring temperature range, changes of slope only take place at temperatures corresponding to  $T_C$  and  $T_I$ . The coincidence of the Curie temperature and the temperature of the first kink during cooling suggests that the phonon softening depends on the magnetic ordering in the sample. It unambiguously affirms that the magnetoelastic coupling plays an important role in the premartensitic transformation and provides direct evidence to support the model predicting the multistage structural transformation by Castán *et al.*<sup>[14]</sup> Above  $T_C$ , magnetoelastic coupling can be understood by the direct interaction between the short-range magnetic fluctuations and the soft phonon potential in the paramagnetic parent state. The degree of phonon softening is enhanced after the material becomes ferromagnetic below  $T_C$ , where the spin system couples to the ionic displacement, producing the magnon-phonon interaction. In addition, both the IF peak and the  $C'$  kink observed at  $T_C$  show a temperature hysteresis, magnified in the inserted sketch of Figure 3. Hence, the transition is not a usual second order one. Instead, it is expected to be a magnetic and elastic transition, which is weakly first order. It has been proposed that an incommensurate phase precedes the premartensitic phase transformation.<sup>[14]</sup> Therefore, it appears reasonable to assume that the weakly first order nature of the Curie transition reflects the entry into the incommensurate phase. A second kink of the

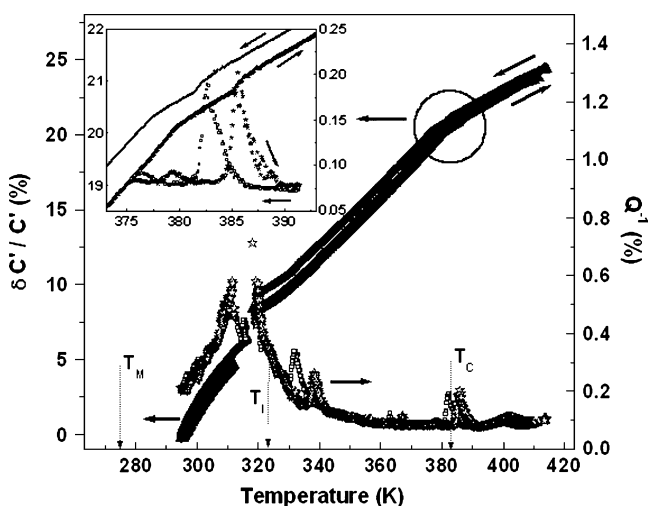


Fig. 3—Evolution of the relative change of the low-frequency  $C'$  and internal friction ( $Q^{-1}$ ) as a function of temperature (cooling and subsequent heating).

low-frequency  $C'$  was detected upon further cooling the specimen to  $T_I$ , where  $C'$  exhibits a discontinuity and a concurrent maximum of the IF. It has been pointed out that the commensurate phase exists in a cubic lattice whose lattice parameter is 3 times larger than the parent phase.<sup>[13]</sup> The maximum of the IF could result from new domain boundaries forming in the commensurate phase.

A few Landau models for the premartensitic transformation in NiMnGa have been proposed.<sup>[8,15]</sup> Considering the magnetoelastic coupling between  $M$ , the magnetization (treated as a scalar here), and  $\eta$ , a plane modulation strain, and between  $M$  and  $\varepsilon$ , a (110) [110] homogeneous shear strain, the free energy can be expressed by

$$F_{\text{general}}(\eta, \varepsilon, M) = F_{\text{shuffle}}(\eta) + F_{\text{shear}}(\varepsilon) + F_{\text{magnetization}}(M) + F_{me}(\eta, \varepsilon, M) \quad [1]$$

where

$$\begin{aligned} F_{\text{shuffle}}(\eta) &= \frac{1}{2}\mu\omega^2\eta^2 + \frac{1}{4}\beta\eta^4 + \frac{1}{6}\gamma\eta^6 \\ F_{\text{shear}}(\varepsilon) &= \frac{1}{2}C'\varepsilon^2 \\ F_{\text{magnetization}}(M) &\approx A(M - M_0)^2 \\ F_{me} &= \frac{1}{2}k_1M^2\eta^2 + \frac{1}{2}k_2M^2\varepsilon^2 \end{aligned} \quad [2]$$

In Eq. [2],  $\omega$  represents the frequency of the soft mode transverse phonon at wave vector  $\langle 1/3, 1/3, 0 \rangle$  and  $C' = (C_{11} - C_{12})/2$ . Both quantities are temperature dependent. Following Planes *et al.*,<sup>[8]</sup> the purely magnetic energy expression  $F_{\text{magnetization}}$  can be linearized around a value  $M_0$  above  $T_I$ , where  $M_0$  denotes the equilibrium magnetization close to the premartensitic transformation. All coefficients in the preceding energy expressions are positive constants.

Minimization of Eq. [1] with respect to  $M$  and  $\varepsilon$  leads to an effective free energy  $F_{\text{eff}}(\eta)$  dependent on  $\eta$  alone:

$$F_{\text{general}}(\eta, \varepsilon, M) = F_{\text{eff}}(\eta) = \frac{1}{2}\mu\tilde{\omega}^2\eta^2 + \frac{1}{4}\tilde{\beta}\eta^4 + \frac{1}{6}\tilde{\gamma}\eta^6 \quad [3]$$

where

$$\tilde{\beta} = \beta - \frac{k_1^2M_0^2}{A} \quad [4]$$

It can thus be seen that the coupling between  $M$  and  $\eta$  leads to  $\tilde{\beta} < 0$  in which case a first-order transition will occur. The elastic anomalies of Ni<sub>49.0</sub>Mn<sub>23.5</sub>Ga<sub>27.5</sub> alloy measured close to  $T_I$  confirm such a weakly first-order transition predicted by the preceding model.

More interestingly, considering the influence of magnetism, the soft phonon frequency is formally given by

$$\omega^2 = a(T - T_I) + b(T - T_C) \quad [5]$$

where  $a$  and  $b$  are positive constants. This relationship indicates that the frequency of the soft mode phonon should exhibit a kink at the Curie temperature, which has been observed by Stühr *et al.*<sup>[11]</sup> The constant  $C'$  can be renormalized in a similar way: according to Eqs. [1] and [2], an effective  $C'_{\text{eff}}$  can be written as

$$\frac{1}{2}C'_{\text{eff}}\varepsilon^2 = \frac{1}{2}C'\varepsilon^2 + \frac{1}{2}k_2M^2\varepsilon^2 \quad [6]$$

Since  $C'$  has been observed to exhibit a linear decrease on cooling to  $T_I$ , it is reasonable to assume that  $C' = p(T - T_I)$ . Further, close to the magnetic ordering temperature, the squared magnetization can be approximated by  $M^2 = q(T - T_C)$  ( $p$  and  $q$  are positive constants in these two expressions). Thus, Eq. [6] can be reduced to

$$C'_{\text{eff}} = p(T - T_I) + q(T - T_C) \quad [7]$$

Equation [7] qualitatively explains the kink of  $C'$  observed at the magnetic ordering temperature in Figure 3. Detailed discussions about the theoretical model of Landau theory applied to the premartensitic phase transformation can be found in References 8 and 15.

In comparison to the information available on all structural transformations, the magnetic properties of NiMnGa in the premartensitic state are less well known. With more and more manifestations of magnetoelastic coupling effects in NiMnGa, magnetic signatures of precursor phenomena are expected to occur.

The magnetization of Ni<sub>49.0</sub>Mn<sub>23.5</sub>Ga<sub>27.5</sub> specimen was determined as a function of temperature between 5 and 390 K. An external 8 kA/m magnetic field was applied along the cubic [110] direction. As shown in Figure 4, the temperatures  $T_C$  and  $T_M$  are well marked by considerable magnetization changes. In addition, a slight increase of the magnetization has been found above 340 K and upon heating to  $T_C$ . This unusual magnetization increase is possibly due to the “lock-in” transition at  $T_I$ . Recalling the well-known facts of phonon stiffening in the commensurate phase below  $T_I$ , it is reasonable that the spins are locked in the commensurate, modulated phase. Therefore, they cannot respond to a small external field. However, the lock-in force is lowered after the material reaches the incommensurate phase on heating so that more and more spins can respond to the applied field. This subtle magnetization change can only be detected in the initial heating curve under an external field smaller than 8 kA/m as the lock-in force in the commensurate phase is expected to be rather weak.

Figure 5(a) displays a series of temperature dependences of the magnetization curves determined in different external fields. During the measurements, the [001] crystallographic direction was oriented parallel to the external field. When the sample was field cooled and heated under a magnetic field smaller than 40 kA/m, a plateau of the magnetization was found between  $T_C$  and  $T_M$ . This effect is consistent with the results of temperature-independent dc susceptibility measurements, plotted in Figure 5(b). Experimentally, the easy direction of magnetization is not known precisely. Webster *et al.*<sup>[20]</sup> proposed that it might be in the

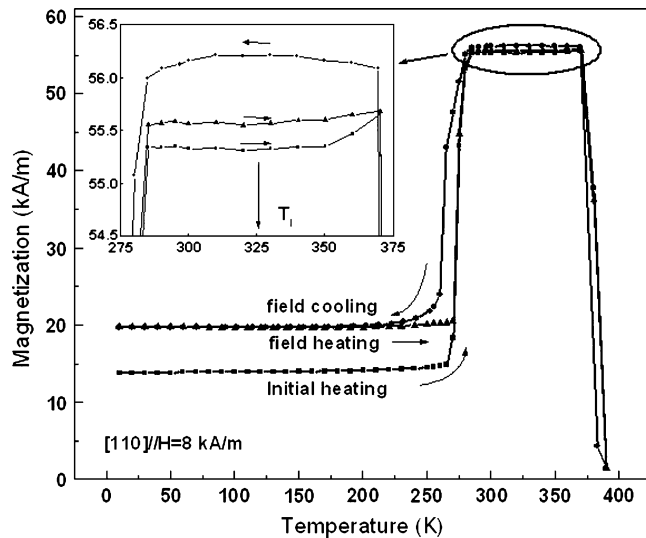


Fig. 4—Temperature dependence of magnetization of  $\text{Ni}_{49.0}\text{Mn}_{23.5}\text{Ga}_{27.5}$  under 8 kA/m magnetic field. The magnetic field is applied parallel to the crystallographic [110] direction of the cubic  $L2_1$  structure. The sample was cooled to 5 K before applying the external field. Subsequently, the initial heating curve was measured in a 8 kA/m field and followed by subsequent field cooling and field heating.

$\langle 111 \rangle$  direction of the  $L2_1$  cubic phase; however, they also mentioned that the difference between the magnetization curves in different orientations is small. Our measurements show that the [001] direction is the easiest direction of magnetization above  $T_M$  (the same as the easy direction in martensite), which will be explicitly demonstrated in the following discussion. This result is in agreement with the published data of Tickle and James in 1999.<sup>[21]</sup> Figure 5(b) also exhibits a finite dc susceptibility of the premartensite phase in NiMnGa, meaning that a non-negligible field is required to magnetically saturate the specimen along the “easy” direction between  $T_C$  and  $T_M$ . This is one of the important characteristics of NiMnGa premartensite that distinguishes it from the classical soft magnetic materials.

The magnetization along the different crystallographic directions of [001], [110], and [111] was measured at various temperatures between  $T_C$  and  $T_M$ . For clarity, only typical magnetization curves at 300 K for fields under  $1.6 \times 10^2$  kA/m are displayed in Figure 6(a). The results show that the material has a small coercivity and the aforementioned finite dc susceptibility. The magnetization curves along all three crystallographic directions exhibit little hysteresis and resemble each other closely. No traditional easy magnetization behavior can be observed along any crystallographic direction of premartensite NiMnGa, although the [001] direction appears to be softer than the other directions. By calculating the difference of the energy  $\int HdM$  of the [001], [110], and [111] magnetization curves at all the measuring temperatures, the temperature dependence of the magnetic anisotropy constants  $K_1$  and  $K_2$  in cubic NiMnGa are obtained and plotted in Figure 6(b). The result indicates that the premartensite NiMnGa has a very low magnetic anisotropy,  $K_1 \approx 10^3$  J/m<sup>3</sup> or less, comparable to that of the magnetically softest amorphous materials.<sup>[22]</sup> The coexistence of finite magnetic dc susceptibility and vanishing magnetic anisotropy is the signature of a

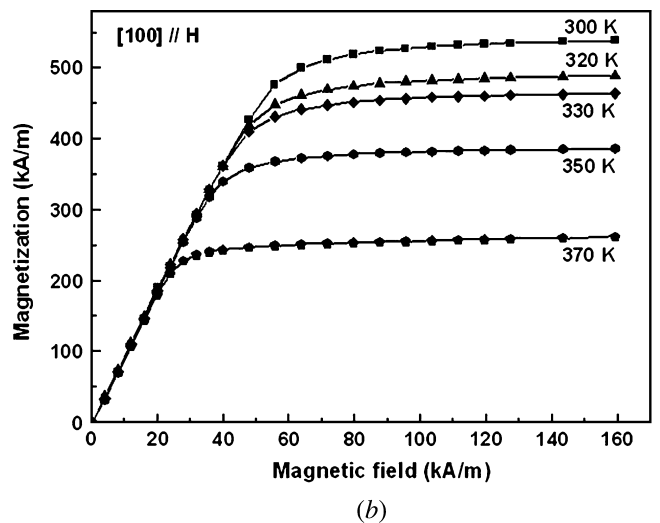
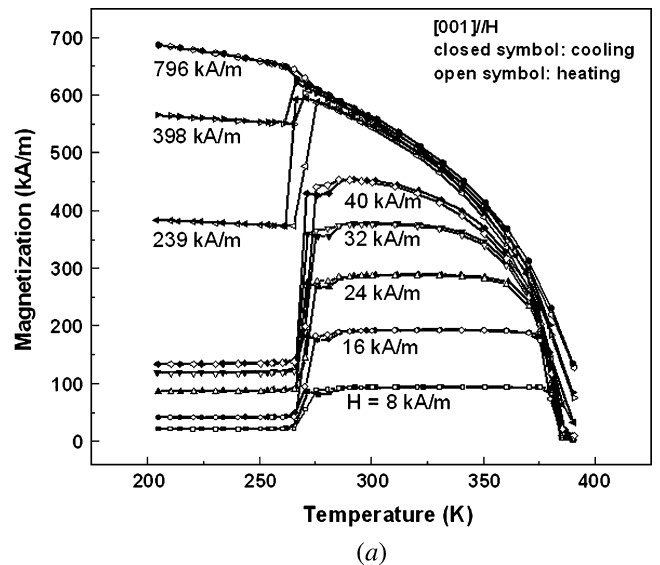
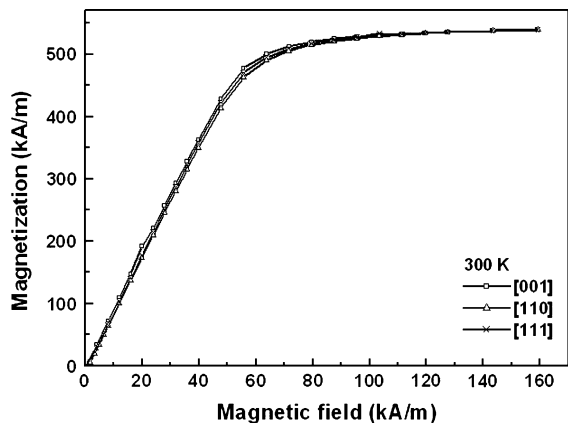


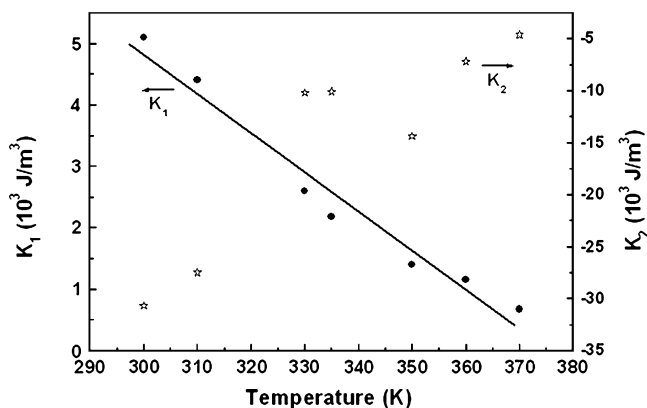
Fig. 5—(a) Temperature dependence of the magnetization of  $\text{Ni}_{49.0}\text{Mn}_{23.5}\text{Ga}_{27.5}$  in various magnetic fields applied parallel to the crystallographic [001] direction of the cubic  $L2_1$  structure. (b) Initial magnetization curves at various temperatures. Magnetic field direction parallel to the cubic [001] direction.

magnetically compensated zero anisotropy state in FSMA NiMnGa alloys. Similar magnetic characteristics were reported for bcc magnetostrictive FeGa<sup>[23]</sup> and fcc FePd.<sup>[24]</sup>

When analyzing the magnetic anisotropy of FeGa alloys containing defect clusters of  $\langle 100 \rangle$  Ga-Ga pairs,<sup>[25]</sup> it was realized that the competition between the coherent crystalline anisotropy,  $K_1$ , and the anisotropy created by the local uniaxial  $\langle 001 \rangle$  pair anisotropies causes an eventual collapse of the magnetic anisotropy. In  $\alpha$ -FeGa,  $\langle 001 \rangle$  Ga-Ga pairs represent the smallest coherent defect that can introduce a local anisotropy field. In NiMnGa, the formation of defects associated with the premartensitic transformation has been confirmed through the diffuse peak of neutron scattering<sup>[10]</sup> and ultrasonic attenuation.<sup>[26]</sup> The local inhomogeneities, including local distorted regions and compositional fluctuations, couple to the soft modes to



(a)



(b)

Fig. 6—(a) Magnetization curves along [001], [110], and [111] directions in  $\text{Ni}_{49.0}\text{Mn}_{23.5}\text{Ga}_{27.5}$  at 300 K. (b) Temperature dependence of magnetic anisotropy constants  $K_1$  and  $K_2$  in bcc  $L2_1$  solids of  $\text{Ni}_{49.0}\text{Mn}_{23.5}\text{Ga}_{27.5}$ .

induce incommensurate nanoclusters (tweed). These clusters produce a locally strong strain field, which is consistent with our observation of the significant peak broadening in the neutron diffraction data. Analysis of the random anisotropy model<sup>[22,25]</sup> (and references therein) indicated that random anisotropy does not cancel out the coherent cubic anisotropy completely, giving rise to the small magnetic anisotropy, as measured in premartensite NiMnGa. It can thus be seen that NiMnGa premartensite has at least two sources of anisotropy, the first being the coherent anisotropy that arises from the transition element host lattice and the second due to the “built-in” crystal-lattice defects of tweed. At sufficiently large defect concentrations, the competition between the coherent and uniaxial defect anisotropy causes a marked decrease of the macroscopic magnetocrystalline anisotropy, as was observed.

#### IV. CONCLUSIONS

Neutron powder diffraction data identify the development of a premartensitic phase in  $\text{Ni}_{49.0}\text{Mn}_{23.5}\text{Ga}_{27.5}$ . Significant peak broadening indicates that a large microstrain is associated with the precursor phenomena. The elastic

constants  $C_{44}$  and  $C'$  display linear behavior with distinct slope changes at the Curie and premartensitic transformation temperatures, supporting the concept of a magnon-phonon coupling enhanced premartensitic transformation. This transition is confirmed to be a weakly first-order transition supported by a discontinuity of the elastic modulus  $C'$ . The formation of the modulated commensurate phase is confirmed by the stiffening of  $C_{44}$  below  $T_I$ . A newly identified magnetically compensated premartensitic state manifests itself through a finite magnetic susceptibility and a vanishing magnetic anisotropy. This behavior is attributed to the competition of a local defect-induced anisotropy and the exchange forces in the ferromagnetic NiMnGa system.

#### ACKNOWLEDGMENTS

We acknowledge the support of the National Institute of Standards and Technology, United States Department of Commerce, in providing the neutron research facilities used in this work. This work was supported by the National Science Foundation, Grant No. DMR0354740, and the Office of Naval Research, Contract Nos. N000140110761 and N000140410085.

#### REFERENCES

1. A.G. Khachatryan, S.M. Shapiro, and S. Semenovskaya: *Phys. Rev. B: Condens. Matter Mater. Phys.*, 1991, vol. 43, pp. 10832-10843.
2. S.M. Shapiro, B.X. Yang, Y. Noda, L.E. Tanner, and D. Schryvers: *Phys. Rev. B: Condens. Matter Mater. Phys.*, 1991, vol. 44, pp. 9301-13.
3. S.M. Shapiro, J.Z. Larese, Y. Noda, S.C. Moss, and L.E. Tanner: *Phys. Rev. Lett.*, 1986, vol. 57, pp. 3199-3202.
4. J.A. Krumhansl and R.J. Gooding: *Phys. Rev. B: Condens. Matter Mater. Phys.*, 1989, vol. 39, pp. 3047-53.
5. A. Sozinov, A.A. Likhachev, and K. Ullakko: *IEEE Trans. Magn.*, 2002, vol. 38, pp. 2814-16.
6. V.A. Chernenko, J. Pons, C. Seguí, and E. Cesari: *Acta Mater.*, 2002, vol. 50, pp. 53-60.
7. X. Jin, M. Marioni, D. Bono, S.M. Allen, R.C. O'Handley, and T.Y. Hsu: *J. Appl. Phys.*, 2002, vol. 91, pp. 8222-24.
8. A. Planes, E. Obradó, A. González-Comas, and L. Mañosa: *Phys. Rev. Lett.*, 1997, vol. 79, pp. 3926-29.
9. L. Manosa, A. González-Comas, E. Obradó, A. Planes, V.A. Chernenko, V.V. Kokorin, and E. Cesari: *Phys. Rev. B: Condens. Matter Mater. Phys.*, 1997, vol. 55, pp. 11068-11071.
10. A. Zheludev, S.M. Shapiro, P. Wochner, A. Schwartz, M. Wall, and L.E. Tanner: *Phys. Rev. B: Condens. Matter Mater. Phys.*, 1995, vol. 51, pp. 11310-14.
11. U. Stühr, P. Vorderwisch, V.V. Kokorin, and P.-A. Lindgård: *Phys. Rev. B: Condens. Matter Mater. Phys.*, 1997, vol. 56, pp. 14360-14365.
12. A. Zheludev, S.M. Shapiro, P. Wochner, and L.E. Tanner: *Phys. Rev. B: Condens. Matter Mater. Phys.*, 1996, vol. 54, pp. 15045-15050.
13. P.J. Brown, J. Crangle, T. Kanomata, M. Matsumoto, K.-U. Nuemann, B. Ouladdiaf, and K.R.A. Ziebeck: *J. Phys. Condens. Matter*, 2002, vol. 14, pp. 10159-10171.
14. T. Castán, A. Planes, and A. Saxena: *Phys. Rev. B*, 2003, vol. 67, pp. 134113-1-6.
15. T. Castán, E. Vives, and P. Lindgård: *Phys. Rev. B: Condens. Matter Mater. Phys.*, 1999, vol. 60, pp. 7071-84.
16. L. Dai, J. Cullen, and M. Wuttig: *J. Appl. Phys.*, 2004, vol. 95, pp. 6957-59.
17. M. Wuttig and C.M. Su: *Proc. Symp. on Damping of Multiphase Inorganic Materials*, R.B. Bhagat, ed., ASM, Metals Park, OH, 1993, pp. 159-63.
18. C.M. Su, Y. Wen, and M. Wuttig: *J. Phys. E*, 1996, vol. 6 (8), pp. 757-68.

19. S.J. Murray, M. Marioni, S.M. Allen, R.C. O'Handley, and T.A. Lograsso: *Appl. Phys. Lett.*, 2000, vol. 77, pp. 886-88.
20. P.J. Webster, K.R.A. Ziebeck, S.L. Town, and M.S. Peak: *Phil. Mag. B*, 1984, vol. 49, pp. 295-310.
21. R. Tickle and R.D. James: *J. Magn. Magn. Mater.*, 1999, vol. 195, pp. 627-38.
22. R. Alben, J.J. Becker, and M.C. Chi: *J. Appl. Phys.*, 1978, vol. 49, pp. 1653-58.
23. H. Rumpf, M. Wuttig, and E. Quandt: Center of Adv. Eur. Studies & Res., Bonn, Germany, 2004, personal communication.
24. J. Cui and R.D. James: *IEEE Trans. Magn.*, 2001, vol. 37, pp. 2675-77.
25. J. Cullen, P. Zhao, and M. Wuttig: *Phys. Rev. Lett.*, 2006, submitted for publication.
26. J. Worgull, E. Petti, and J. Trivisonno: *Phys. Rev. B: Condens. Matter Mater. Phys.*, 1996, vol. 54, pp. 15695-15699.